ORIGINAL PAPER
Polish Journal of Microbiology
2022, Vol. 71, No 2, 161–171
https://doi.org/10.33073/pjm-2022-015

# Growth Behavior and Transcriptome Profile Analysis of *Proteus mirabilis* Strain Under Long- versus Short-Term Simulated Microgravity Environment

BIN ZHANG[1]*, PO BAI[2] and DAPENG WANG[3]

[1] Department of Respiratory and Critical Care Medicine, Binzhou Medical University Hospital, Binzhou, China
[2] Respiratory Diseases Department, PLA Rocket Force Characteristic Medical Center, Beijing, China
[3] Respiratory Diseases Department, The Second Medical Center of PLA General Hospital, Beijing, China

Submitted 31 December 2021, accepted 7 March 2022, published online 23 May 2022

Abstract

Spaceflight missions affect the behavior of microbes that are inevitably introduced into space environments and may impact astronauts' health. Current studies have mainly focused on the biological characteristics and molecular mechanisms of microbes after short-term or long-term spaceflight, but few have compared the impact of various lengths of spaceflight missions on the characteristics of microbes. Researchers generally agree that microgravity (MG) is the most critical factor influencing microbial physiology in space capsules during flight missions. This study compared the growth behavior and transcriptome profile of *Proteus mirabilis* cells exposed to long-term simulated microgravity (SMG) with those exposed to short-term SMG. The results showed that long-term SMG decreased the growth rate, depressed biofilm formation ability, and affected several transcriptomic profiles, including stress response, membrane transportation, metal ion transportation, biological adhesion, carbohydrate metabolism, and lipid metabolism in contrast to short-term SMG. This study improved the understanding of long-term versus short-term SMG effects on *P. mirabilis* behavior and provided relevant references for analyzing the influence of *P. mirabilis* on astronaut health during spaceflights.

Keywords: *Proteus mirabilis*, simulated microgravity, length of time, phenotype, transcriptomics

## Introduction

The field of space life science has become a new research frontier following the advent of space exploration and the development of space technology (Belobrajdic et al. 2021; Macaulay et al. 2021). During space exploration, microbes are inevitably introduced into space habitats by astronauts and may grow on surfaces in the space capsule (Singh et al. 2018; Checinska Sielaff et al. 2019). Due to extreme environmental factors, such as microgravity (MG), high vacuum, and intense radiation, microbes in space undergo a series of changes in gene expression at the transcriptional level and eventually perform global physiological alterations, including metabolism, growth rate, motility, virulence, and biofilm formation (Taylor 2015; Senatore et al. 2018). For instance, strains of *Candida albicans* exposed to a short-duration spaceflight showed enhanced cell aggregation and random budding under the differential expression of transcriptional regulators involved in oxidative stress resistance, aggregation, and random budding (Crabbé et al. 2013). *Escherichia coli* strains grew at higher antibiotic concentrations within 49 h of being cultured in a space environment compared to the Earth and differentially expressed genes (DEGs) related to starvation and oxidative stress responses (Aunins et al. 2018). *Acinetobacter baumannii* subjected to long-duration spaceflight showed decreased biofilm formation ability than the ground controls, coinciding with down-regulated type IV pili-related genes (Zhao et al. 2018). Overall, these data strongly suggest that microbes' biological characteristics and molecular mechanisms were affected during or immediately following spaceflights, regardless of mission duration. However, much less is known regarding the precise impact of different mission durations on microbial growth behavior and transcriptome profiles.

* Corresponding authors: B. Zhang, Department of Respiratory and Critical Care Medicine, Binzhou Medical University Hospital, Binzhou, China; **e-mail: zhangbin19840531@163.com**
© 2022 Bin Zhang et al.
This work is licensed under the Creative Commons Attribution-NonCommercial-NoDerivatives 4.0 License (https://creativecommons.org/licenses/by-nc-nd/4.0/).

MG is defined as a state of weightlessness that occurs due to decreased physical force exerted by gravity, where gravity ranges from $10^{-3}$ to $10^{-6}$ *g* (Bijlani et al. 2020). There is general agreement that MG is a crucial factor influencing microbial physiology in the space capsule during flight missions (Tesei et al. 2021). Due to technological and logistical hurdles, the microbial experiments under true MG in space stations are minimal. Therefore, different types of ground-based bioreactors, such as clinostats, rotating wall vessels (RWVs), and random positioning machines (RPMs), have been designed to develop a simulated microgravity (SMG) environment to analyze microbial responses to space MG (Acres et al. 2021). A high aspect ratio vessel (HARV) is a typical RWV that creates a low-fluid shear and weightless environment by revolving around an axis perpendicular to the gravitational vector (Sheet et al. 2019). Specifically, it simulates the true MG environment of spaceflight and has been used extensively to analyze the physiological response of bacteria to SMG (Hauserman et al. 2021). Since the invention of the HARV, the effects of SMG have been studied in several microbial species including *E. coli*, *Pseudomonas aeruginosa*, and *Staphylococcus aureus* (Crabbé et al. 2010; Castro et al. 2011; Tirumalai et al. 2019).

Moreover, several studies have shown that results obtained from HARV experiments are similar to those obtained in a true MG. For example, *Salmonella* Typhimurium cultivated in a true MG environment showed increased virulence in mice and revealed a role for its global regulator Hfq (Wilson et al. 2007). This phenomenon was shown due to a prior ground-based experiment that utilized the HARV and had previously produced similar results (Nickerson et al. 2000).

*Proteus mirabilis* is a common opportunistic pathogen frequently isolated from patients with urinary tract infections (UTIs), particularly in the elderly population at nursing homes and patients undergoing long-term catheterization (Matthews and Lancaster 2011; Armbruster et al. 2018). This pathogen primarily differentiates into elongated swarm forms, migrates to the epithelial cells of the urinary tract, and finally induces UTIs (Armbruster et al. 2012). In addition, *P. mirabilis* expresses fimbriae to mediate catheter attachment and biofilm maturation, which protects bacteria from the host immune response and the antibiotic inhibitory effect (Fusco et al. 2017). *P. mirabilis* has already been found in samples from human space habitats or post-flight astronauts, and it is likely to induce infectious diseases in the space environment given that the immune system of astronauts is significantly impaired during spaceflight (Klaus and Howard 2006; Crucian et al. 2018). Therefore, it is necessary to study the biological characteristics and genetic features of *P. mirabilis* in MG. To date, multiomics analysis has already been developed to study the molecular mechanisms of microbial survival and adaption in MG and SMG environments (Milojevic and Weckwerth 2020). Although a recent study has analyzed the phenotype and transcriptome of *P. mirabilis* after short-term exposure to SMG, long-term SMG exposure and varying lengths of SMG exposure to *P. mirabilis* remain unclear (Wang et al. 2021). In this study, the growth behavior and transcriptome profile of *P. mirabilis* exposed to long-term SMG were compared with those exposed to short-term SMG to analyze the effect of MG exposure duration on its characteristics. This study is expected to improve the understanding of long-term versus short-term SMG on *P. mirabilis* and provide relevant references for analyzing the influence of *P. mirabilis* on astronaut health during spaceflights.

## Experimental

### Materials and Methods

**Bacterial strain and culture conditions.** The original *P. mirabilis* strain, used in this study, was obtained from the Space Biomedical Laboratory of the Second Medical Center of the Chinese PLA General Hospital and has already been described many times (Wang et al. 2021). The strain was cultivated at 37°C for 24 h under constant shaking (200 rpm) in Luria-Bertani (LB) medium.

**HARV experiment.** The bacterial culture was adjusted to a turbidity of 1.0 and inoculated at 1:100 in the HARV bioreactor chambers (Synthecon Inc., USA). The chambers were filled with the culture medium, and air bubbles in the chambers were carefully removed through valves. The bacterial cultures were grown in rotated chambers around the horizontal axis at 37°C with a rotation rate of 25 rpm (Fig. 1). After 24 h, the

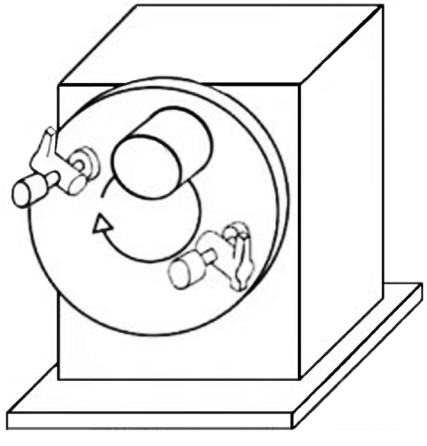

Fig. 1. Schematic diagram of mechanical principle of HARV. MG is simulated by rotating the samples around a plane perpendicular to the gravity vector.

bacterial cultures were poured out from the chambers, diluted to a turbidity of 1.0, and added into the new chambers at a volume ratio of 1:100 in LB medium. The bacterial suspension was cultivated at 37°C and 25 rpm for another 24 h. Experimental operations of bacterial inoculation in the chambers of HARV bioreactors were successively repeated three times for three days (short-term exposure to SMG, designated as PMS) and 21 times for three weeks (long-term exposure to SMG, designated as PML).

**Growth rate assay.** The growth rates of PML and PMS were determined using the Bioscreen C system and BioLink software (Lab Systems, Finland). Approximately, 200 µl of PMS and PML was taken from each chamber at every 2 h interval on the 3rd day and 21st day, respectively. Then the samples were inoculated into a 96-well microtiter plate. The growth rates of PML and PMS were monitored by measuring the optical density at 600 nm ($OD_{600}$) every 2 h. A blank well containing 200 µl of LB medium was used as a negative control. This experiment was performed in three replicates.

**Biofilm formation assay.** About 200 µl of each sample was added to a 96-well honeycomb microtiter plate and statically cultivated at 37°C for 24 h. After removing unattached cells with PBS, the 96-well microtiter plate was cultured at a temperature of 80°C for 15 min to fix the biofilm. The adhered cells were stained with 200 µl of 0.1% crystal violet for 15 min. Subsequently, the 96-well microtiter plate was washed with PBS and dried for another 10 min. Finally, the stained wells were dissolved in 95% ethanol to digest the biofilm, and the optical density at 570 nm ($OD_{570}$) for each well was measured using a Thermo Multiskan Ascent (Thermo, USA). This experiment was performed in three replicates.

**Swarming motility assay.** The swarming motility of *P. mirabilis* was analyzed using Petri dishes containing a swarming medium (0.5% agar, 0.5% glucose, and 0.8% nutrient broth). Bacterial cultures were adjusted to a $10^8$ CFU/ml density and inoculated in the dishes using a sterile needle. After incubation at 37°C for 24 h, the swarming motility of the strains was determined by measuring the diameter of the circular turbid zone formed by the bacterial suspension migrating away from the point of inoculation. This experiment was performed in three replicates.

**RNA extraction, cDNA synthesis, and sequencing.** The exponential growth phase of samples was determined according to the growth curves, and cultures at the exponential phase were used for transcriptome analysis. Briefly, total RNAs of samples were extracted by TRIZOL and purified using RNeasy Mini Kit (Qiagen, German) following the manufacturer's instructions. The quality and quantity of RNAs were checked by capillary electrophoresis (Agilent Bioanalyzer 2100, USA) and with a spectrophotometer (Nanodrop 2000, USA). The RIN/RQN values ranged from 8.2 to 9.5. Subsequently, the ribosomal RNA (rRNA) was removed from the total RNA using a Ribo-Zero RNA Removal Kit (Illumina, USA). The purified RNA samples were then subjected to cDNA library construction using TruSeqTM Stranded Total RNA Library Prep Kit (Illumina, USA). Fragmentation buffer was added to cleave the mRNA into ~ 200 bp fragments, and the fragments were reverse transcribed into the first strand of cDNA by random primer. The second strand of cDNA was synthesized using DNA polymerase I and RNase H. Next, the samples were resolved with the End Repair Mix for end repair and Poly (A) addition for adapter ligation. After adapter ligation, the second strand of cDNA was degraded by the UNG enzyme, and the suitable fragments were selected for PCR amplification. Finally, TBS380 (Picogreen) samples were quality-checked and sequenced using Illumina HiSeq System.

**Read processing, alignment, and quantification.** All raw reads for RNA-seq were filtered, and clean reads were obtained by removing reads with adaptors, unknown nucleotides ≥ 5%, and low-quality bases (< Q10) number ≥ 20%. The RNA-seq reads were then mapped to the reference genome (*P. mirabilis* HI4320) using HISAT and Bowtie tools. The gene expression levels of each sample were analyzed using RESM software. Gene expression values were calculated using FPKM. Differential gene expression was analyzed using the DESeq2 method, and genes with $\log_2$ (FoldChange) ≥ 1 and adjusted $p$-value ≤ 0.05 were defined as differentially expressed genes (DEGs). The function of each DEG was analyzed using the Kyoto Encyclopedia of Gene and Genomes (KEGG) database.

**Data and statistical analyses**. Phenotypic experiments and RNA sequencing were conducted in triplicate and the values were represented as mean ± standard deviation. A statistical comparison of data was evaluated by the two-tailed Student's $t$-test. Statistical significance between PML and PMS was defined as $p < 0.05$.

## Results

**The growth rate of PML versus PMS.** The growth rates of PML and PMS were measured, and growth rate data are shown in Table I. When grown in LB medium, the maximum specific growth rates of PML and PMS were 0.167 $h^{-1}$ and 0.196 $h^{-1}$, respectively. In terms of growth ability, PML exhibited a lower $OD_{600}$ value than PMS, suggesting that growth ability decreased with increasing SMG exposure time (Fig. 2).

**Biofilm formation ability of PML versus PMS.** The biofilm formation ability of PML and PMS was assessed by the crystal violet staining, and optical density at 570 nm ($OD_{570}$) was measured for each strain

Table I
$OD_{600}$ value of PML and PMS.

| Time (h) | PML | PMS |
|---|---|---|
| 0 | 0.548 ± 0.005 | 0.547 ± 0.006 |
| 2 | 0.581 ± 0.008 | 0.591 ± 0.005 |
| 4 | 0.674 ± 0.010 | 0.726 ± 0.005 |
| 6 | 0.863 ± 0.026 | 0.955 ± 0.012 |
| 8 | 1.206 ± 0.018 | 1.411 ± 0.026 |
| 10 | 1.560 ± 0.022 | 1.636 ± 0.013 |
| 12 | 1.709 ± 0.019 | 1.806 ± 0.027 |
| 14 | 1.776 ± 0.016 | 1.872 ± 0.024 |
| 16 | 1.826 ± 0.021 | 1.938 ± 0.025 |
| 18 | 1.876 ± 0.018 | 1.983 ± 0.015 |
| 20 | 1.927 ± 0.018 | 1.955 ± 0.014 |
| 22 | 1.900 ± 0.019 | 1.957 ± 0.028 |
| 24 | 1.889 ± 0.018 | 1.916 ± 0.014 |

to determine the quantity of the biofilm. The results showed that PML decreased the $OD_{570}$ value in contrast to PMS (0.096 ± 0.006 vs. 0.118 ± 0.011, $p = 0.032$), suggesting that the biofilm formation ability of the strain decreased as SMG exposure time increased (Fig. 3).

**Swarming motility of PML versus PMS.** The swarming motility of PML and PMS was determined by measuring the diameter of the circular turbid zone formed by the strains on the Petri dishes. The results showed that a similar circular zone developed in PML and PMS (33.667 ± 3.215 mm vs. 37.333 ± 0.058 mm, $p = 0.124$), suggesting that swarming motility of the strain was unchanged with increasing exposure time to SMG (Fig. 4).

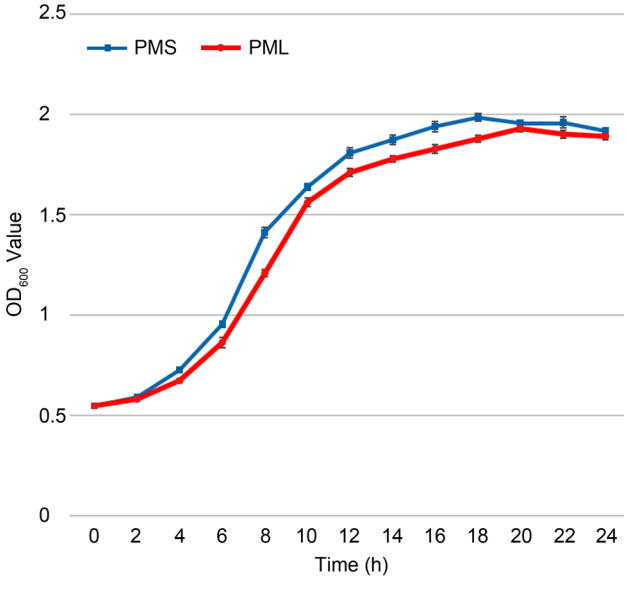


Fig. 2. Growth curve of PML (red) and PMS (blue). The growth curves of PML and PMS were quantified by measuring the $OD_{600}$ values every 2 h for 24 h.

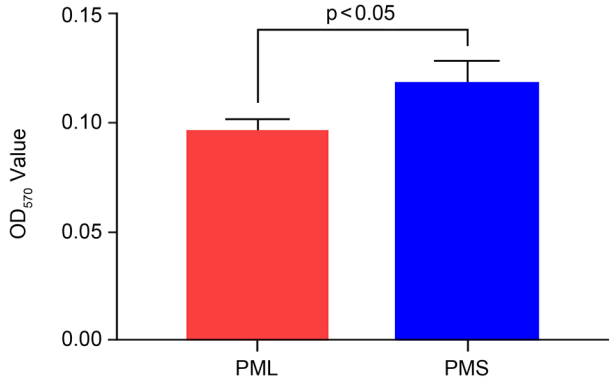


Fig. 3. Biofilm formation ability of PML (red) and PMS (blue). Biofilm formation ability of PML and PMS was examined by measuring the $OD_{570}$ values in microtiter plates.

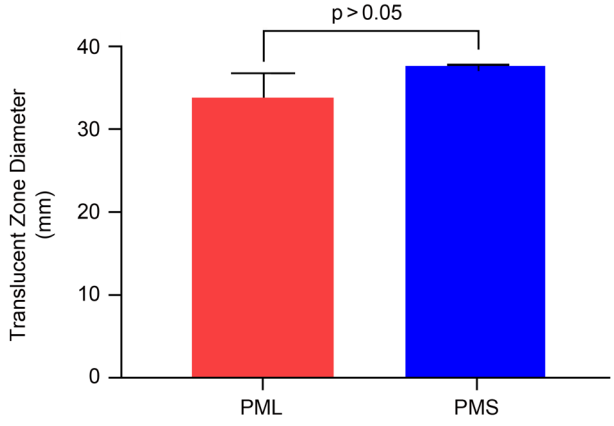


Fig. 4. Swarming motility of PML (red) and PMS (blue). Swarming motility of PML and PMS was determined by measuring the translucent zone diameters in swarming agar.

**Transcriptome profile analysis of PML versus PMS.** Comparative transcriptomic analysis of PML and PMS was performed to reveal the impact of different time lengths of SMG on the molecular characteristics of the strain. The accession number of transcriptomic data for PML is SAMN23475021 and SAMN23509825, and for PMS is SAMN23498564. The percentage of total reads for PML and PMS mapped to the reference strain *P. mirabilis* HI4320 were 94.31% and 95.36%, respectively. The correlation of gene expression levels between PML and PMS was evaluated using the Pearson correlation coefficient. In this study, the $R^2$ between samples was 0.987, suggesting that the sample selection was reasonable and that the findings were reliable. A Venn diagram of common and specific genes in PML and PMS is shown in Fig. 5. A total of 3,085 common genes were identified in both PML and PMS, while 16 and 12 specific genes were detected in PML and PMS, respectively.

DEGs were determined using the criteria of abs $\log_2$ (FoldChange) ≥ 1 and adjusted $p$-value ≤ 0.05. As shown in Table II, a total of 50 genes were differentially expressed between PML and PMS, including 19 upregulated

Table II
Statistics of differentially expressed genes (DEGs).

| Gene ID | Expression (up/down) | $Log_2$ FoldChang (PML/PMS) | Adjusted *p*-value | Gene products |
|---|---|---|---|---|
| *csdA* | up | 1.308 | < 0.001 | cysteine sulfinate desulfinase |
| *csdE* | up | 1.156 | < 0.001 | cysteine desulfuration protein |
| *cutC* | up | 1.323 | 0.004 | choline trimethylamine-lyase |
| *phoA* | up | 1.686 | 0.002 | alkaline phosphatase |
| *pspA* | up | 1.077 | 0.003 | phage shock protein A |
| *pspB* | up | 1.107 | 0.002 | phage shock protein B |
| *pstB* | up | 1.423 | 0.049 | phosphate transport system ATP-binding protein |
| *rplT* | up | 1.060 | 0.023 | large subunit ribosomal protein |
| *ugpA* | up | 1.439 | 0.002 | phosphate transport system ATP-binding protein |
| *ugpB* | up | 1.377 | < 0.001 | phosphate transport system ATP-binding protein |
| *ugpC* | up | 1.228 | 0.010 | phosphate transport system ATP-binding protein |
| *ugpE* | up | 1.575 | 0.002 | phosphate transport system ATP-binding protein |
| *PMI_RS02645* | up | 1.148 | < 0.001 | fimbria/pilus periplasmic chaperon |
| *PMI_RS09180* | up | 1.031 | 0.022 | cysteine desulfurase |
| *PMI_RS09250* | up | 1.064 | 0.009 | sensor histidine kinase |
| *PMI_RS13360* | up | 2.720 | < 0.001 | small multidrug resistance pump |
| *PMI_RS13370* | up | 1.424 | 0.017 | putative phosphotransacetylase |
| *PMI_RS14325* | up | 1.473 | 0.023 | amino acid transport system substrate-binding protein |
| *PMI_RS17915* | up | 1.520 | < 0.001 | $Cd^{2+}/Zn^{2+}$-exporting ATPase |
| *artP* | down | −1.009 | < 0.001 | arginine transport system ATP-binding protein |
| *cyoB* | down | −1.290 | 0.022 | cytochrome o ubiquinol oxidase subunit I |
| *epd* | down | −1.011 | 0.007 | D-erythrose 4-phosphate dehydrogenase |
| *fadB* | down | −1.330 | 0.016 | 3-hydroxyacyl-CoA dehydrogenase |
| *fadE* | down | −1.045 | 0.047 | acyl-CoA dehydrogenase |
| *feoA* | down | −1.277 | < 0.001 | ferrous iron transport protein A |
| *glpA* | down | −1.465 | 0.005 | glycerol-3-phosphate dehydrogenase |
| *glpB* | down | −1.348 | 0.023 | glycerol-3-phosphate dehydrogenase |
| *glpT* | down | −1.221 | 0.003 | glycerol-3-phosphate transporter |
| *ilvN* | down | −1.080 | 0.018 | acetolactate synthase I/III small subunit |
| *metI* | down | −1.178 | 0.003 | D-methionine transport system permease protein |
| *msrB* | down | −1.021 | < 0.001 | peptide-methionine oxide reductase |
| *phsA* | down | −1.181 | 0.046 | thiosulfate reductase |
| *ptsG* | down | −1.099 | < 0.001 | PTS system, glucose-specific IIB component |
| *PMI_RS00340* | down | −1.105 | < 0.001 | protein NrfC |
| *PMI_RS00505* | down | −1.210 | 0.048 | cytochrome ubiquinol oxidase subunit III |
| *PMI_RS00510* | down | −1.283 | 0.036 | cytochrome ubiquinol oxidase subunit IV |
| *PMI_RS07940* | down | −1.255 | 0.028 | – |
| *PMI_RS09930* | down | −1.008 | 0.048 | toxin CptA |
| *PMI_RS10955* | down | −2.137 | < 0.001 | major pilin subunit PapA |
| *PMI_RS13425* | down | −1.001 | < 0.001 | phosphorelay signal transduction system |
| *PMI_RS13430* | down | −1.190 | < 0.001 | TetR/AcrR family transcriptional regulator |
| *PMI_RS14090* | down | −1.029 | < 0.001 | putative transport protein |
| *PMI_RS14825* | down | −1.315 | 0.017 | Mat/Ecp fimbriae adhesion |
| *PMI_RS14830* | down | −1.430 | 0.012 | Mat/Ecp fimbriae outer membrane usher protein |
| *PMI_RS14835* | down | −1.349 | 0.037 | Mat/Ecp fimbriae periplasmic chaperone |
| *PMI_RS14840* | down | −2.151 | 0.048 | Mat/Ecp fimbriae adhesion |
| *PMI_RS15035* | down | −1.003 | 0.027 | cation/acetate symporter |
| *PMI_RS15880* | down | −1.250 | < 0.001 | glycerol uptake facilitator protein |
| *PMI_RS17135* | down | −1.018 | 0.020 | minor fimbrial subunit |
| *PMI_RS18425* | down | − 1.060 | 0.023 | putative oxidoreductase |

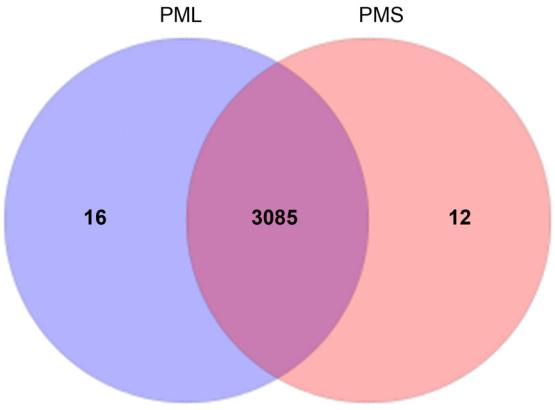


Fig. 5. The Venn diagram of common and specific genes in PML and PMS.

genes and 31 downregulated genes. A scatter plot of PML versus PMS is shown in Fig. 6.

Fourteen categories, including 50 DEGs (identical DEGs may fall into different categories), were identified between PML and PMS according to the KEGG pathway classification (Fig. 7). Compared with PMS, PML is characterized by regulating genes related to cellular community, membrane transport, energy metabolism, carbohydrate metabolism, lipid metabolism, and amino acid metabolism.

Notably, some DEGs were found to belong to diverse functional categories including stress response (*pspAB*, *msrB*, *PMI_RS13425*), membrane transportation (*artP*, *metI*, *pstB*, *ugpABCE*, *PMI_RS14325*), metal

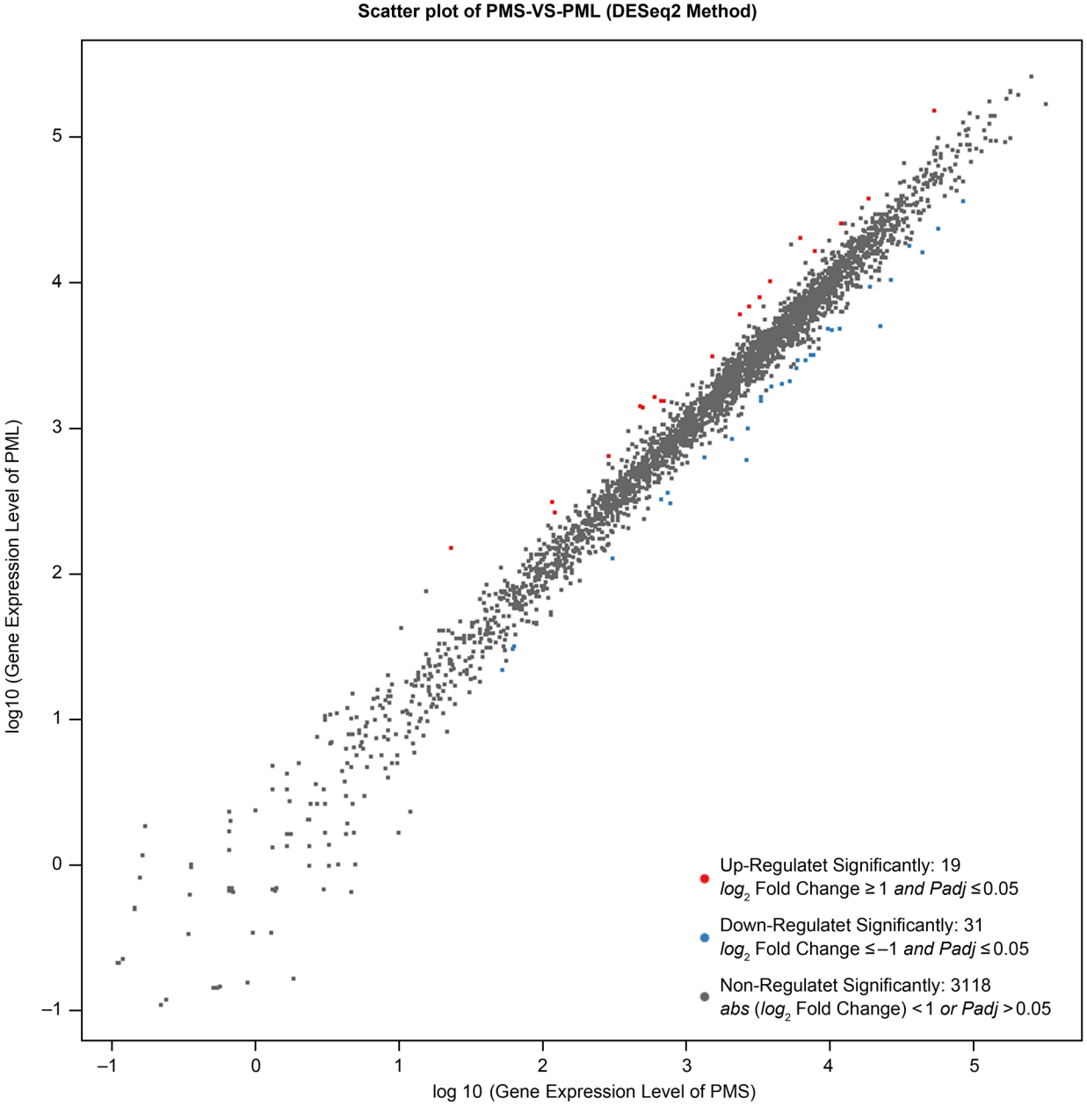


Fig. 6. Scatter plot of DEGs. The x-axis and y-axis represent the logarithm of the gene expression for PML and PMS, respectively. Red spots and blue spots represent upregulated and downregulated genes, respectively.

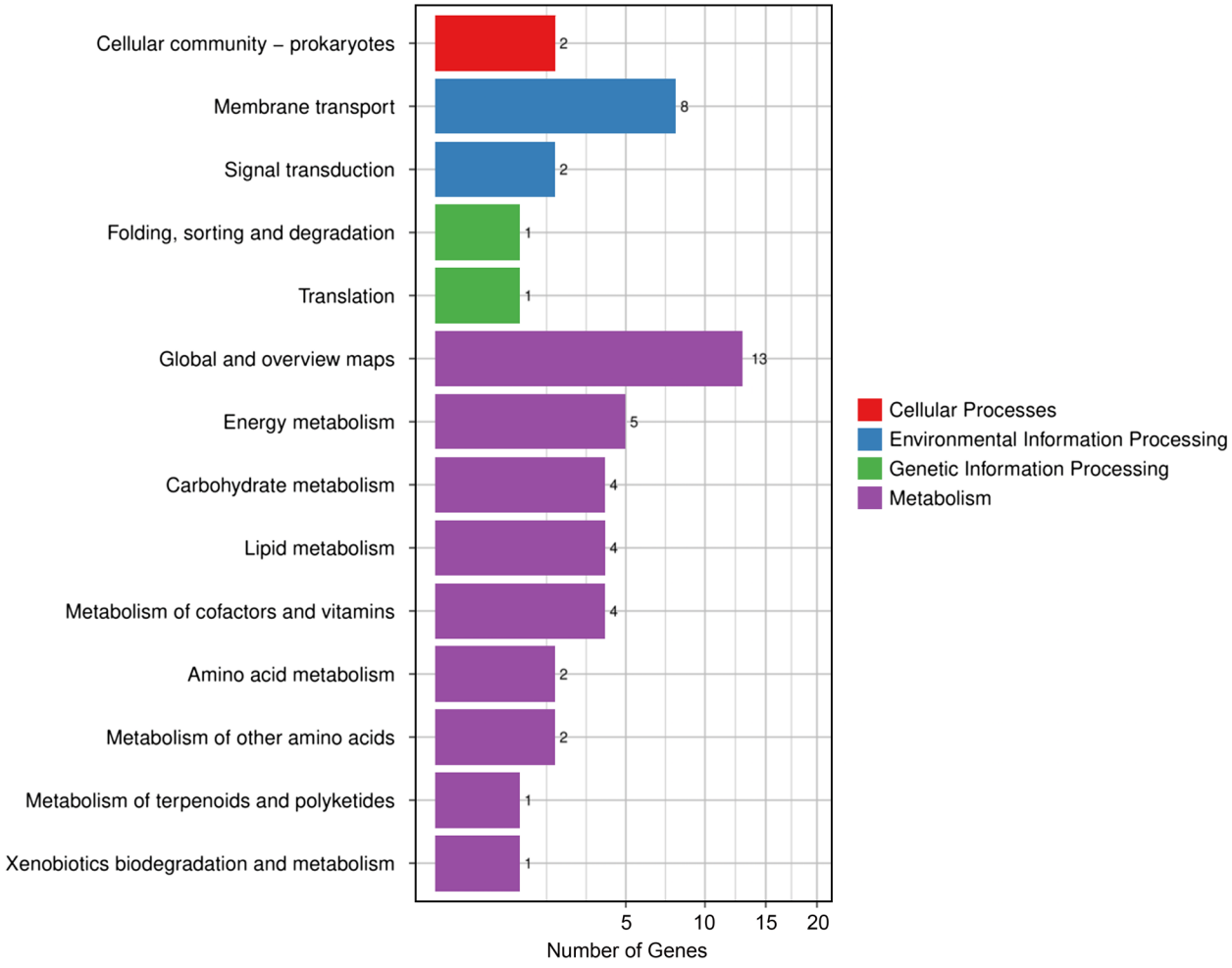


Fig. 7. KEGG pathway analysis of DEGs. The x-axis and y-axis represent the numbers of DEGs and KEGG pathway category, respectively.

ion transportation (*feoA*, *PMI_RS14090*, *PMI_RS15035*, *PMI_RS17915*), biological adhesion (*PMI_RS02645*, *PMI_RS10955*, *PMI_RS14825*, *PMI_RS14830*, *PMI_RS14835*, *PMI_RS14840*, *PMI_RS17135*), carbohydrate metabolism (*fadB*, *ilvN*, *ptsG*, *PMI_RS13370*), and lipid metabolism (*fadBE*, *glpAB*) and selected for further analysis between PML and PMS. The variation between PML and PMS at the transcriptomic level might lead to physiological changes in *P. mirabilis* and help bacteria survive better in a prolonged SMG environment.

## Discussion

It is the first study to analyze the growth behavior and transcriptome profile of *P. mirabilis* exposed to long-term versus short-term SMG. The results showed that *P. mirabilis* exhibited a decreased growth rate and impaired biofilm formation ability under long-term SMG compared to short-term SMG. Further transcriptomic profiling demonstrated that the relevant molecular mechanisms of physiological alteration might be attributed to the differential expression of genes associated with membrane transportation, metal ion transportation, carbohydrate metabolism, lipid metabolism, and biological adhesion. This study improved the understanding of the various lengths of MG exposure on *P. mirabilis* behavior and provided relevant references for analyzing the influence of *P. mirabilis* on astronaut health during spaceflights.

The effects of MG on the growth rate and final cell density of microorganisms are controversial. Previous studies have shown that microorganisms have an increased growth rate, with a growth curve characterized by a shorter lag phase and a more prolonged exponential phase under MG or SMG. For example, *C. albicans* has been reported to have a slightly shorter generation time and higher growth propensity in spaceflights than those cultivated under NG (Nielsen et al. 2021). Similarly, another experiment demonstrated that *Lactobacillus acidophilus* showed a shorter lag phase and faster growth rate in the early stage of SMG in HARVs (Shao et al. 2017). Another study showed that the final cell population of *Vibrio natriegens* (Garschagen et al. 2019)

increased significantly under SMG using a clinostat. A common explanation is that the lack of sedimentation occurring in MG led to a uniform distribution of cells with abundant utilization of nutrients, enabling denser microbial growth (Senatore et al. 2018). However, a contrasting study reported that *S. aureus* exhibited a reduced growth rate under SMG compared to NG (Hauserman et al. 2021). A recent experiment also showed that *E. coli* showed a decreased growth profile under SMG compared with that under NG, and the growth difference might be due to several factors involved in cell fitness (Yim et al. 2020). Following the above, a flight mutant strain of *Bacillus cereus* was found to have a decreased growth rate compared with the ground control, which may have been due to downregulated genes involved in lipid biosynthesis and energy transportation (Su et al. 2014). In addition, some experiments demonstrated that microbes grown in SMG or space conditions did not differ in growth rate cell size and shape from the controls. Researchers reported no significant differences in final $OD_{600}$ for *Rhodospirillum rubrum* between the SMG and the control samples (Mastroleo et al. 2013). An experiment focused on *Lactobacillus reuteri* showed no difference in the growth rate and cell size between two SMG systems and normal gravity controls (Senatore et al. 2020). Recently, an investigation conducted on the ISS focused on *Cupriavidus metallidurans*, *Bacillus subtilis*, and *Sphingomonas desiccabilis*. The experiment verified the effect of different gravity regimens on the final cell density of all bacteria on the ISS, and no differences in final cell count and optical density were identified within any of the three strains despite different sedimentation rates (Santomartino et al. 2020). The most plausible explanation was that all species had reached the stationary phase, leading to a similar cell count for each bacterial species. In this study, the $OD_{600}$ value of cell cultures was used to determine the growth rate of *P. mirabilis* under different SMG exposure durations, and the strain grew slower in long-term versus short-term SMG environments. The results suggested that *P. mirabilis* decreased its growth ability with increasing exposure time to SMG. The overlap of several factors caused the growth variation, and the downregulated genes involved in lipid metabolism, carbohydrate metabolism, and metal ion transportation might take an essential role in the decreased growth ability of the long-term SMG exposure strain.

Biofilms produced by microbes in the water system and device surface of the spacecraft cabin represent a significant phenotype concerning virulence and antibiotic resistance and induce corrosion of metals and structural materials (Novikova et al. 2006; Liu 2017). Therefore, it is necessary to analyze the biofilm formation ability of microbes under real and simulated MG. A representative investigation demonstrated that the biofilm of *P. aeruginosa* exhibited an atypical structure composed of columns overlapped with a canopy during spaceflights, which has not been observed on Earth (Kim et al. 2013). During short-term spaceflight, enhanced biofilm formation was also observed in *Klebsiella pneumoniae* (Li et al. 2014). The SMG environment also influences the biofilm formation ability of microbes by providing low shear forces of cellular fluid (Yamaguchi et al. 2014). For example, *K. pneumoniae* grown under SMG in HARVs exhibited increased biofilm formation compared to those grown under NG after two weeks of subculture, and the overexpressed genes related to type 3 fimbriae (*mrkABCDF*)-mediated biofilm formation on abiotic surfaces (Wang et al. 2016). Similarly, in a more recent experiment, *Stenotrophomonas maltophilia* cultivated under SMG in HARVs also produced more biofilm biomass than those under NG condition after two weeks of subculture, and upregulated genes responsible for type 4 fimbriae (*pilAG*) participated in this process (Su et al. 2021). In this study, the biofilm formation ability of the two groups was quantified using the $OD_{570}$ values of crystal violet staining. The results showed that *P. mirabilis* under long-term SMG exposure decreased its biofilm formation ability compared with the identical strain under short-term SMG exposure, suggesting that *P. mirabilis* impaired its biofilm formation ability with increasing exposure time to SMG. Further transcriptomic profiling revealed that some genes related to fimbriae adhesion were downregulated under long-term versus short-term SMG. *P. mirabilis* encodes 17 putative chaperone-usher fimbrial operons and the role of five fimbriae, including urothelial cell adhesin (UCA), *P. mirabilis* fimbria (PMF), mannose resistant *Proteus*-like (MR/P), ambient temperature fimbria (ATF), and *P. mirabilis*-like pili (PMP), has been clearly identified (Pearson et al. 2008). It has been reported that *P. mirabilis* fimbriae have different roles in biofilm generation, and the UCA and PMF mutants improved biofilm formation ability compared to the wild-type strain, whereas the MR/P and ATF mutants formed significantly less biofilm than the wild-type strain (Scavone et al. 2016). Therefore, we preliminarily concluded that the downregulated genes encoded by other chaperone-usher fimbrial operons first decreased the activity of Mat/Ecp fimbriae protein, subsequently impairing biological adhesion and finally reducing the biofilm formation ability of *P. mirabilis* with increasing exposure time to SMG.

Motility is a critical microbial behavior that plays a crucial role in nutrient absorption, tissue localization and invasion, biofilm formation, virulence, and survival (Acres et al. 2021). Alterations in microbial motility often originate from changes in the gene expression of the flagella-related system (Morgenstein et al. 2010). Although few studies have focused explicitly

on the effects of spaceflight and SMG on the phenotype of microbial motility, genetic and transcriptomic analyses have provided a general understanding of gene expression that can predict microbial motility according to the genes involved in flagella function (Milojevic and Weckwerth 2020). *E. coli* cultured in minimal MOPS medium upregulated its motility genes (*fliCDZ* and *flgBDEK*) in HARVs compared with NG rotation (Tucker et al. 2007). Consistent with this, *P. aeruginosa* cultured in LB medium also overexpressed motility genes, including *fliACDGS, fleLNP*, and *flgM* in HARVs in contrast to NG (Crabbé et al. 2010). In opposite, *Salmonella* Typhimurium grown in LB medium exhibited downregulated expression of flagellar genes, including *fimA* and *fliB,* in HARVs compared with NG rotation (Wilson et al. 2002). In this study, no significant difference in the flagella-related genes at the transcriptomic level was detected between long-term and short-term SMG exposure, and swarming motility of *P. mirabilis* was unchanged with increasing exposure time to SMG.

## Conclusion

This study presents the only data available to compare long-term versus short-term SMG exposure effects on *P. mirabilis* cultured in HARVs. The results indicate that *P. mirabilis* modified its growth behavior to better adapt to the SMG environment with increasing exposure time. The transcriptomic analysis provides a practical and comprehensive strategy for identifying the effects of different lengths of SMG exposure on biological processes and pathways. This phenomenon may help understand how microbes adapt to spaceflight missions over different durations.

China's space station will be completed in the early 2020s, and spaceflight missions will require astronauts to remain on the space station for long periods. With the reality of long-duration missions lasting years, avoiding infectious diseases induced by microbes and maintaining the safety of the space station are of great significance in the future. Due to the challenges of sending microbial samples into the space environment, most research still needs to be done in laboratories using ground-based bioreactors under SMG. Considering that one of the new challenges facing astronauts is reaching increasingly long-duration spaceflight targets, studying the influences of long-term versus short-time SMG exposure on the growth behavior of *P. mirabilis* is necessary to predict possible pathogenesis mechanisms and develop treatments for infectious diseases under spaceflight conditions. In the future, more studies are needed to establish a space microbiological safety assessment system to protect crew members and ensure the safe operation of space stations.

**Acknowledgments**

This study was sponsored by the scientific research foundation program of Binzhou Medical University (No. BY2020KYQD39).

**Conflict of interest**

The authors do not report any financial or personal connections with other persons or organizations, which might negatively affect the contents of this publication and/or claim authorship rights to this publication.

## Literature

**Acres JM, Youngapelian MJ, Nadeau J.** The influence of spaceflight and simulated microgravity on bacterial motility and chemotaxis. NPJ Microgravity. 2021 Feb;7(1):7.
https://doi.org/10.1038/s41526-021-00135-x

**Armbruster CE, Mobley HLT, Pearson MM.** Pathogenesis of *Proteus mirabilis* infection. EcoSal Plus. 2018 Feb;8(1):10.1128/ecosalplus.ESP-0009-2017.
https://doi.org/10.1128/ecosalplus.ESP-0009-2017

**Armbruster CE, Mobley HL.** Merging mythology and morphology: the multifaceted lifestyle of *Proteus mirabilis*. Nat Rev Microbiol. 2012 Nov;10(11):743–754.
https://doi.org/10.1038/nrmicro2890

**Aunins TR, Erickson KE, Prasad N, Levy SE, Jones A, Shrestha S, Mastracchio R, Stodieck L, Klaus D, Zea L, et al.** Spaceflight modifies *Escherichia coli* gene expression in response to antibiotic exposure and reveals role of oxidative stress response. Front Microbiol. 2018 Mar;9:310.
https://doi.org/10.3389/fmicb.2018.00310

**Belobrajdic B, Melone K, Diaz-Artiles A.** Planetary extravehicular activity (EVA) risk mitigation strategies for long-duration space missions. NPJ Microgravity. 2021 May;7(1):16.
https://doi.org/10.1038/s41526-021-00144-w

**Bijlani S, Stephens E, Singh NK, Venkateswaran K, Wang CCC.** Advances in space microbiology. iScience. 2021 Apr;24(5):102395.
https://doi.org/10.1016/j.isci.2021.102395

**Castro SL, Nelman-Gonzalez M, Nickerson CA, Ott CM.** Induction of attachment-independent biofilm formation and repression of *hfq* expression by low-fluid-shear culture of *Staphylococcus aureus*. Appl Environ Microbiol. 2011 Sep;77(18):6368–6378.
https://doi.org/10.1128/AEM.00175-11

**Checinska Sielaff A, Urbaniak C, Mohan GBM, Stepanov VG, Tran Q, Wood JM, Minich J, McDonald D, Mayer T, Knight R, et al.** Characterization of the total and viable bacterial and fungal communities associated with the International Space Station surfaces. Microbiome. 2019 Apr;7(1):50.
https://doi.org/10.1186/s40168-019-0666-x

**Crabbé A, Pycke B, Van Houdt R, Monsieurs P, Nickerson C, Leys N, Cornelis P.** Response of *Pseudomonas aeruginosa* PAO1 to low shear modelled microgravity involves AlgU regulation. Environ Microbiol. 2010 Jun;12(6):1545–1564.
https://doi.org/10.1111/j.1462-2920.2010.02184.x

**Crabbé A, Nielsen-Preiss SM, Woolley CM, Barrila J, Buchanan K, McCracken J, Inglis DO, Searles SC, Nelman-Gonzalez MA, Ott CM, et al.** Spaceflight enhances cell aggregation and random budding in *Candida albicans*. PLoS One. 2013 Dec;8(12):e80677.
https://doi.org/10.1371/journal.pone.0080677

**Crucian BE, Choukèr A, Simpson RJ, Mehta S, Marshall G, Smith SM, Zwart SR, Heer M, Ponomarev S, Whitmire A, et al.** Immune system dysregulation during spaceflight: potential countermeasures for deep space exploration missions. Front Immunol. 2018 Jun;9:1437. https://doi.org/10.3389/fimmu.2018.01437

**Fusco A, Coretti L, Savio V, Buommino E, Lembo F, Donnarumma G.** Biofilm formation and immunomodulatory activity of *Proteus mirabilis* clinically isolated strains. Int J Mol Sci. 2017 Feb; 18(2):414. https://doi.org/10.3390/ijms18020414

**Garschagen LS, Mancinelli RL, Moeller R.** Introducing *Vibrio natriegens* as a microbial model organism for microgravity research. Astrobiology. 2019 Oct;19(10):1211–1220. https://doi.org/10.1089/ast.2018.2010

**Hauserman MR, Rice KC.** Growth of *Staphylococcus aureus* using a rotary cell culture system. In: Rice KC, editor. *Staphylococcus aureus*. Methods in Molecular Biology. New York (USA): Humana; 2021. p. 79–88. https://doi.org/10.1007/978-1-0716-1550-8_10

**Kim W, Tengra FK, Young Z, Shong J, Marchand N, Chan HK, Pangule RC, Parra M, Dordick JS, Plawsky JL, et al.** Spaceflight promotes biofilm formation by *Pseudomonas aeruginosa*. PLoS One. 2013 Apr;8(4):e62437. https://doi.org/10.1371/journal.pone.0062437

**Klaus DM, Howard HN.** Antibiotic efficacy and microbial virulence during space flight. Trends Biotechnol. 2006 Mar;24(3):131–136. https://doi.org/10.1016/j.tibtech.2006.01.008

**Li J, Liu F, Wang Q, Ge P, Woo PC, Yan J, Zhao Y, Gao GF, Liu CH, Liu C.** Genomic and transcriptomic analysis of NDM-1 *Klebsiella pneumoniae* in spaceflight reveal mechanisms underlying environmental adaptability. Sci Rep. 2014 Aug;4:6216. https://doi.org/10.1038/srep06216

**Liu C.** The theory and application of space microbiology: China's experiences in space experiments and beyond. Environ Microbiol. 2017 Feb;19(2):426–433. https://doi.org/10.1111/1462-2920.13472

**Macaulay TR, Peters BT, Wood SJ, Clément GR, Oddsson L, Bloomberg JJ.** Developing proprioceptive countermeasures to mitigate postural and locomotor control deficits after long-duration spaceflight. Front Syst Neurosci. 2021 Apr;15:658985. https://doi.org/10.3389/fnsys.2021.658985

**Mastroleo F, Van Houdt R, Atkinson S, Mergeay M, Hendrickx L, Wattiez R, Leys N.** Modelled microgravity cultivation modulates N-acylhomoserine lactone production in *Rhodospirillum rubrum* S1H independently of cell density. Microbiology. 2013 Dec; 159(Pt_12): 2456–2466. https://doi.org/10.1099/mic.0.066415-0

**Matthews SJ, Lancaster JW.** Urinary tract infections in the elderly population. Am J Geriatr Pharmacother. 2011 Oct;9(5):286–309. https://doi.org/10.1016/j.amjopharm.2011.07.002

**Milojevic T, Weckwerth W.** Molecular mechanisms of microbial survivability in outer space: A systems biology approach. Front Microbiol. 2020 May;11:923. https://doi.org/10.3389/fmicb.2020.00923

**Morgenstein RM, Szostek B, Rather PN.** Regulation of gene expression during swarmer cell differentiation in *Proteus mirabilis*. FEMS Microbiol Rev. 2010 Sep;34(5):753–763. https://doi.org/10.1111/j.1574-6976.2010.00229.x

**Nielsen S, White K, Preiss K, Peart D, Gianoulias K, Juel R, Sutton J, McKinney J, Bender J, Pinc G, et al.** Growth and antifungal resistance of the pathogenic yeast, *Candida Albicans*, in the microgravity environment of the International Space Station: An aggregate of multiple flight experiences. Life (Basel). 2021 Mar;11(4):283. https://doi.org/10.3390/life11040283

**Nickerson CA, Ott CM, Mister SJ, Morrow BJ, Burns-Keliher L, Pierson DL.** Microgravity as a novel environmental signal affecting *Salmonella enterica* serovar Typhimurium virulence. Infect Immun. 2000 Jun;68(6):3147–3152. https://doi.org/10.1128/IAI.68.6.3147-3152.2000

**Novikova N, De Boever P, Poddubko S, Deshevaya E, Polikarpov N, Rakova N, Coninx I, Mergeay M.** Survey of environmental biocontamination on board the International Space Station. Res Microbiol. 2006 Jan-Feb;157(1):5–12. https://doi.org/10.1016/j.resmic.2005.07.010

**Pearson MM, Sebaihia M, Churcher C, Quail MA, Seshasayee AS, Luscombe NM, Abdellah Z, Arrosmith C, Atkin B, Chillingworth T, et al.** Complete genome sequence of uropathogenic *Proteus mirabilis*, a master of both adherence and motility. J Bacteriol. 2008 Jun;190(11):4027–4037. https://doi.org/10.1128/JB.01981-07

**Santomartino R, Waajen AC, de Wit W, Nicholson N, Parmitano L, Loudon CM, Moeller R, Rettberg P, Fuchs FM, Van Houdt R, et al.** No effect of microgravity and simulated mars gravity on final bacterial cell concentrations on the International Space Station: applications to space bioproduction. Front Microbiol. 2020 Oct;11:579156. https://doi.org/10.3389/fmicb.2020.579156

**Scavone P, Iribarnegaray V, Caetano AL, Schlapp G, Härtel S, Zunino P.** Fimbriae have distinguishable roles in *Proteus mirabilis* biofilm formation. Pathog Dis. 2016 Jul;74(5):ftw033. https://doi.org/10.1093/femspd/ftw033

**Senatore G, Mastroleo F, Leys N, Mauriello G.** Effect of microgravity and space radiation on microbes. Future Microbiol. 2018 Jun; 13:831–847. https://doi.org/10.2217/fmb-2017-0251

**Senatore G, Mastroleo F, Leys N, Mauriello G.** Growth of *Lactobacillus reuteri* DSM17938 under two simulated microgravity systems: Changes in reuterin production, gastrointestinal passage resistance, and stress genes expression response. Astrobiology. 2020 Jan;20(1):1–14. https://doi.org/10.1089/ast.2019.2082

**Shao D, Yao L, Riaz MS, Zhu J, Shi J, Jin M, Huang Q, Yang H.** Simulated microgravity affects some biological characteristics of *Lactobacillus acidophilus*. Appl Microbiol Biotechnol. 2017 Apr; 101(8):3439–3449. https://doi.org/10.1007/s00253-016-8059-6

**Sheet S, Sathishkumar Y, Choi MS, Lee YS.** Insight into *Pseudomonas aeruginosa* pyocyanin production under low-shear modeled microgravity. Bioprocess Biosyst Eng. 2019 Feb;42(2):267–277. https://doi.org/10.1007/s00449-018-2031-z

**Singh NK, Wood JM, Karouia F, Venkateswaran K.** Succession and persistence of microbial communities and antimicrobial resistance genes associated with International Space Station environmental surfaces. Microbiome. 2018 Nov;6(1):204. https://doi.org/10.1186/s40168-018-0585-2

**Su L, Zhou L, Liu J, Cen Z, Wu C, Wang T, Zhou T, Chang D, Guo Y, Fang X, et al.** Phenotypic, genomic, transcriptomic and proteomic changes in *Bacillus cereus* after a short-term space flight. Adv Space Res. 2014 Jan; 53:18–29. https://doi.org/10.1016/j.asr.2013.08.001

**Su X, Guo Y, Fang T, Jiang X, Wang D, Li D, Bai P, Zhang B, Wang J, Liu C.** Effects of simulated microgravity on the physiology of *Stenotrophomonas maltophilia* and multiomic analysis. Front Microbiol. 2021 Aug;12:701265. https://doi.org/10.3389/fmicb.2021.701265

**Taylor PW.** Impact of space flight on bacterial virulence and antibiotic susceptibility. Infect Drug Resist. 2015 Jul;8:249–262. https://doi.org/10.2147/IDR.S67275

**Tesei D, Chiang AJ, Kalkum M, Stajich JE, Mohan GBM, Sterflinger K, Venkateswaran K.** Effects of simulated microgravity on the proteome and secretome of the polyextremotolerant black fungus *Knufia chersonesos*. Front Genet. 2021 Mar;12:638708. https://doi.org/10.3389/fgene.2021.638708

**Tirumalai MR, Karouia F, Tran Q, Stepanov VG, Bruce RJ, Ott CM, Pierson DL, Fox GE.** Evaluation of acquired antibiotic resistance in *Escherichia coli* exposed to long-term low-shear modeled microgravity and background antibiotic exposure. mBio. 2019 Jan;10(1):e02637-18. https://doi.org/10.1128/mBio.02637-18

**Tucker DL, Ott CM, Huff S, Fofanov Y, Pierson DL, Willson RC, Fox GE.** Characterization of *Escherichia coli* MG1655 grown in a low-shear modeled microgravity environment. BMC Microbiol. 2007 Mar;7:15. https://doi.org/10.1186/1471-2180-7-15

**Wang D, Bai P, Zhang B, Su X, Jiang X, Fang T, Wang J, Liu C.** Decreased biofilm formation in *Proteus mirabilis* after short-term exposure to a simulated microgravity environment. Braz J Microbiol. 2021 Dec;52(4):2021–2030.
https://doi.org/10.1007/s42770-021-00588-y

**Wang H, Yan Y, Rong D, Wang J, Wang H, Liu Z, Wang J, Yang R, Han Y.** Increased biofilm formation ability in *Klebsiella pneumoniae* after short-term exposure to a simulated microgravity environment. Microbiologyopen. 2016 Oct;5(5):793–801.
https://doi.org/10.1002/mbo3.370

**Wilson JW, Ramamurthy R, Porwollik S, McClelland M, Hammond T, Allen P, Ott CM, Pierson DL, Nickerson CA.** Microarray analysis identifies *Salmonella* genes belonging to the low-shear modeled microgravity regulon. Proc Natl Acad Sci USA. 2002 Oct; 99(21):13807–13812. https://doi.org/10.1073/pnas.212387899

**Wilson JW, Ott CM, Höner zu Bentrup K, Ramamurthy R, Quick L, Porwollik S, Cheng P, McClelland M, Tsaprailis G, Radabaugh T, et al.** Space flight alters bacterial gene expression and virulence and reveals a role for global regulator Hfq. Proc Natl Acad Sci USA. 2007 Oct;104(41):16299–16304.
https://doi.org/10.1073/pnas.0707155104

**Yamaguchi N, Roberts M, Castro S, Oubre C, Makimura K, Leys N, Grohmann E, Sugita T, Ichijo T, Nasu M.** Microbial monitoring of crewed habitats in space-current status and future perspectives. Microbes Environ. 2014 Sep;29(3):250–260.
https://doi.org/10.1264/jsme2.me14031

**Yim J, Cho SW, Kim B, Park S, Han YH, Seo SW.** Transcriptional profiling of the probiotic *Escherichia coli* Nissle 1917 strain under simulated microgravity. Int J Mol Sci. 2020 Apr;21(8):2666.
https://doi.org/10.3390/ijms21082666

**Zhao X, Yu Y, Zhang X, Huang B, Bai P, Xu C, Li D, Zhang B, Liu C.** Decreased biofilm formation ability of *Acinetobacter baumannii* after spaceflight on China's Shenzhou 11 spacecraft. Microbiology Open. 2019 Jun;8(6):e00763. https://doi.org/10.1002/mbo3.763